Electronic supplementary information

On-Chip Refractive Index Cytometry for Whole-Cell Deformability Discrimination

Antoine Leblanc-Hotte,[*a] Nadine Sen Nkwe,[b] Geneviève Chabot-Roy,[c] El Bachir Affar,[b] Sylvie Lesage,[cd] Jean-Sébastien Delisle,[efg] and Yves-Alain Peter [a]

[a] Department of Engineering Physics, Polytechnique Montreal, Montreal, QC H3T 1J4, Canada.
E-mail: antoine.leblanc-hotte@polymtl.ca
[b] Maisonneuve-Rosemont Hospital Research Center, Department of Medicine, University of Montreal, Montreal, QC H1T 2M4, Canada
[c] Cellular Immunogenetics Laboratory, Maisonneuve-Rosemont Hospital Research Center, Montreal, QC H1T 2M4, Canada
[d] Département de microbiologie, infectiologie et immunologie, University of Montreal, Montreal, QC H3C 3J7, Canada
[e] Cancer and Transplantation Immunology Laboratory, Maisonneuve-Rosemont Hospital Research Center, Montreal, QC H1T 2M4, Canada
[f] Department of Medicine, University of Montreal, Montreal, QC H3C 3J7, Canada
[g] Hemato-oncology service, Maisonneuve-Rosemont Hospital, Montreal, QC H1T 2M4, Canada

Examples of numerical simulation curve

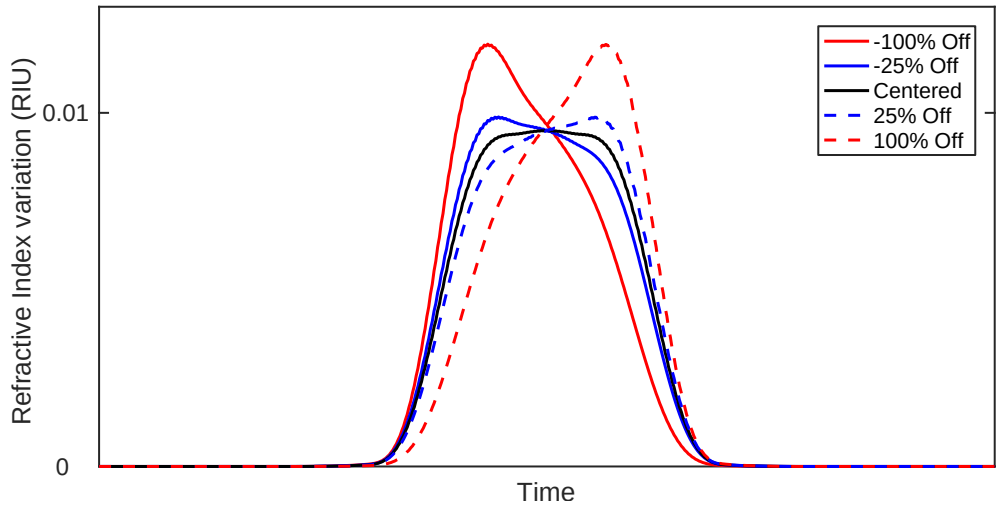

Fig. S1 Examples of numerically simulated RI variation curve for different relative positions of the nucleus.

The measured optical power curve showed in Fig. 3 of the manuscript are in good agreement with this effective RI numerical simulation over time. Indeed, output curve are predominantly shaped by the resonance peak shift dynamics, which is itself dictated by the effective RI variation in time.

The mismatch between the simulated RI variation curve and the measured losses vs time can be justified by the lack of light-matter interaction phenomenon considered by the numerical model. Indeed, the simulation algorithm does not take into account the absorption, diffraction or lens effect of the different parts of the cell. Also, the slope of the resonance peak in the spectrum is not linear and thus will also mold the measured losses curve. Still, this RI variation numerical model gives a good understanding of how the deformation of the cell and the relative position of the nucleus affect the measured curve.

Inertial focusing length and cells spread

The required length for complete inertial focusing in a two-stage scheme as reported by Zhou and Papautsky is:

$$L = \frac{3\pi\mu D_h^2}{4\rho U_f D_{cell}^3}\left(\frac{H}{C_L^-} + \frac{W}{C_L^+}\right) \quad \text{for} \quad W > H$$

where μ and ρ are the fluid viscosity and density respectively, $D_h = 2WH/(W+H)$ is the hydraulic diameter, H and W are the channel height and width respectively, U_f is the average fluid velocity, D_{cell} is the cell diameter and C_L^- and C_L^+ are the negative and positive lift coefficient respectively. Using the data provided by Zhou and Papautsky, the lift coefficients can be approximated.[1] This form is generally more restrictive (outputs longer lengths) than the one proposed by Di Carlo.[2] The table below reports the lift coefficients, the required focusing lengths and the resulting spreads in width W_{spread} for a cavity placed 1.2 mm away from the beginning of the straight channel. Importantly, the cross-section dimensions for cells to be focused are $H - D_{cell}$ and $W - D_{cell}$ in height and width respectively. Also, the calculated spread in width includes the cells diameters as shown in Fig. S2.

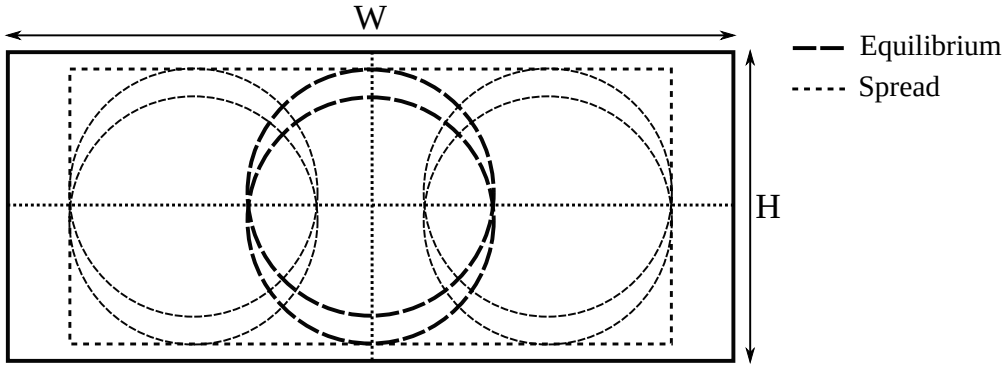

Fig. S2 Inertial equilibrium positions in a rectangular channel and focusing area due to the spread in width.

Table S1 Calculated lift coefficients, required focusing lengths and resulting spreads in width for a cavity placed 1.2 mm away from the beginning of the straight channel for cells of 12 μm in a $W = 40\ \mu m$ by $H = 15\ \mu m$ channel at different flow rates.

Flow rate Q (μl/min)	C_L^-	C_L^+	L (mm)	W_{spread}
5	0.47	0.048	2.7	27.9
10	0.21	0.026	2.6	27.2
15	0.14	0.018	2.5	26.8
20	0.1	0.014	2.5	26.5
30	0.06	0.009	2.4	26.1

Table S2 Calculated lift coefficients, required focusing length and resulting spread in width for a cavity placed 1.2 mm away from the beginning of the straight channel for cells of 12 μm in a $W = 30\ \mu m$ by $H = 15\ \mu m$ channel at 15 μl/min.

Flow rate Q (μl/min)	C_L^-	C_L^+	L (mm)	W_{spread}
15	0.11	0.015	1.2	12.5

Curve parameters dependencies to relative nucleus position

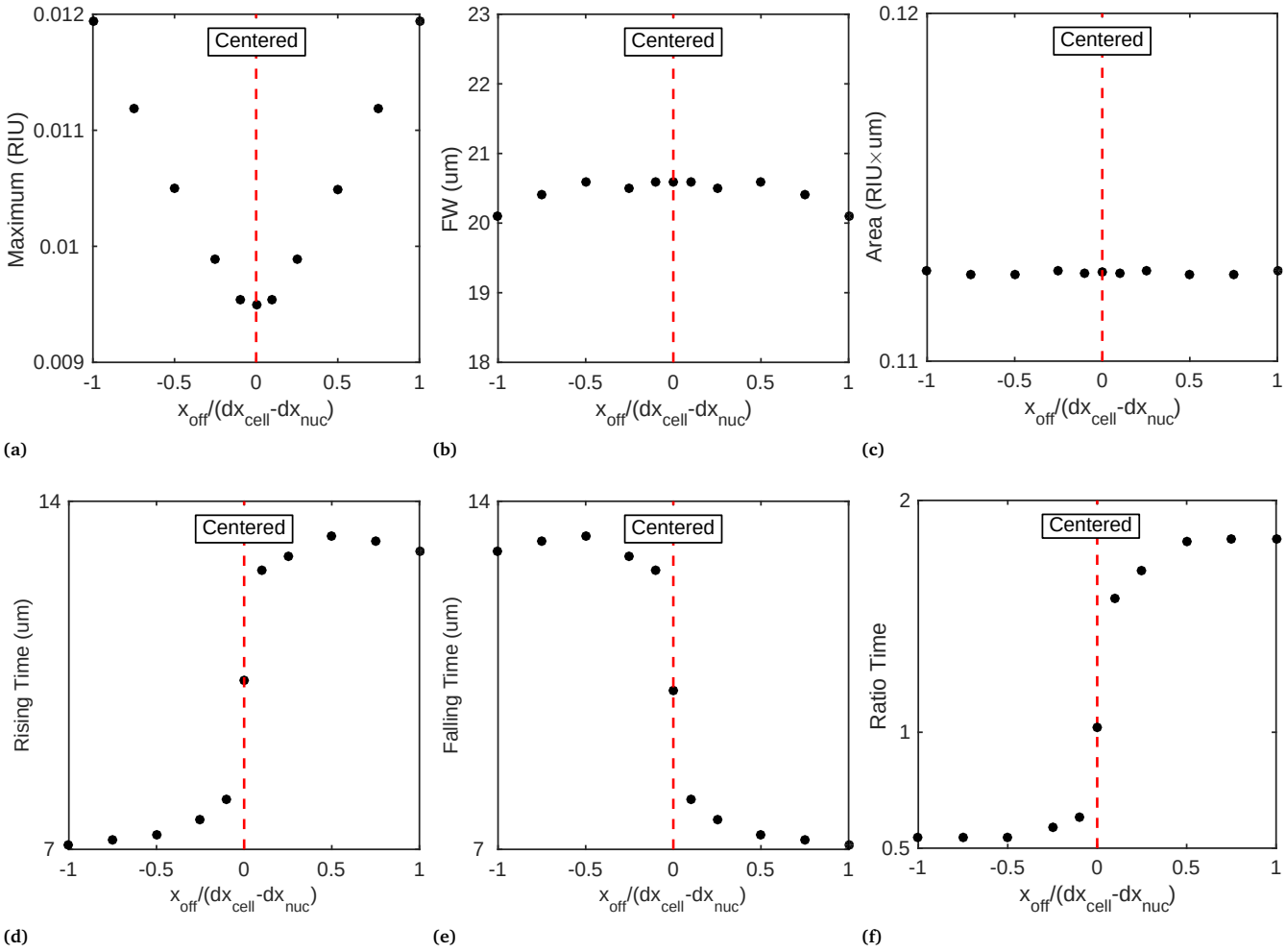

Fig. S3 Computed parameter values from simulated curve when varying the relative nucleus position for (a) max, (b) full width (FW), (c) area, (d) rising time (RT), (e) falling time (FT) and (f) ratio time. Red dashed lines indicates a centered nucleus position. Each steps are 25% offset except for the two points closest to the centered position which are $\pm$10%.

Curve parameters dependencies to deformed cell length

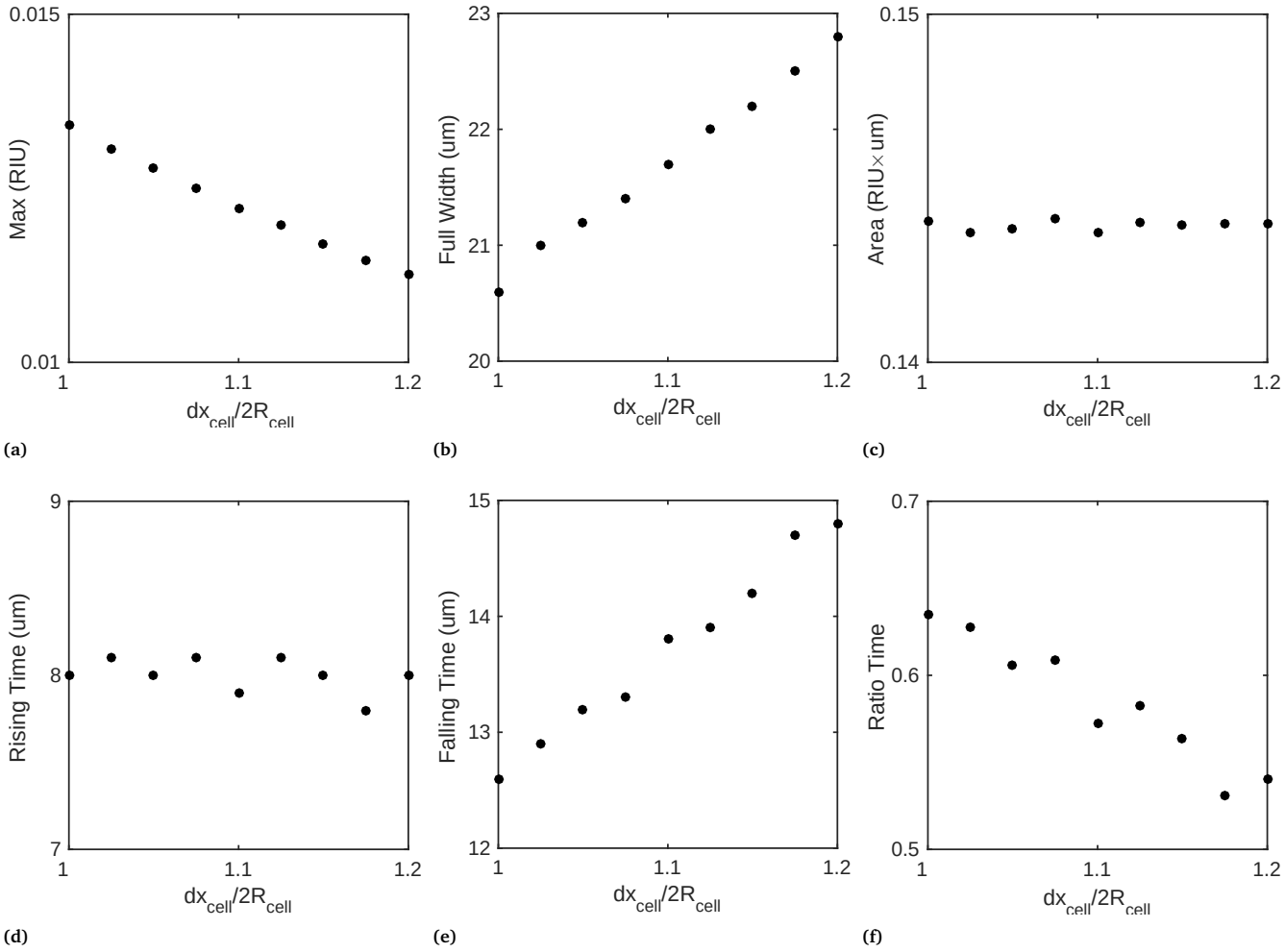

Fig. S4 Computed parameter values from simulated curve when varying the deformed cell length in the x-axis for (a) max, (b) full width (FW), (c) area, (d) rising time (RT), (e) falling time (FT) and (f) ratio time. Deformed cell length is $dx_{cell}/2R_{cell}$ where dx_{cell} is the diameter of the cell ellipsoid in the x-axis. A fixed 10% contraction deformation was imposed on the cell membrane ellipsoid in the y-axis. The nucleus radius was matched to the one of the cell in the y-axis by a 0.9% contraction deformation. For each step of 2.5% deformation, both the cell and the nucleus ellipsoids were deformed in the x-axis. The nucleus relative position was kept at $x_{off}/(dx_{cell} - dx_{nuc}) = -0.5$. Other nucleus relative position yielded similar results.

Confocal microscopy

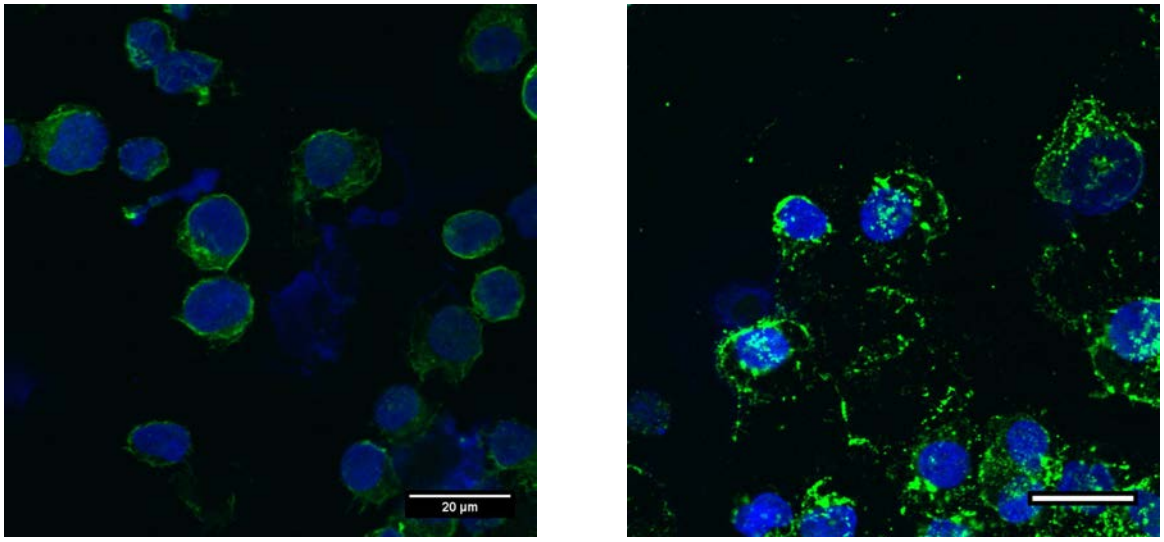

(a) (b)

Fig. S5 Confocal fluorescence microscopy images of cytospun immunostained control and cytochalasin B treated HL-60 cells. F-actin is stained with Alexa Fluor 488 phalloidin (green) and nuclei is stained with DAPI (blue). Top view of the fluorescence composite for (a) HL-60 cells control and (b) cytochalasin B treated HL-60 cells. Treated cells present clumps of phalloidine fluorescence associated to grouped broken-down actin filaments, responsible for the larger whole-cell deformability. Scale bars are 20 μm.

Flow cytometry measurement of control and cytochalasin B treated HL-60 cells

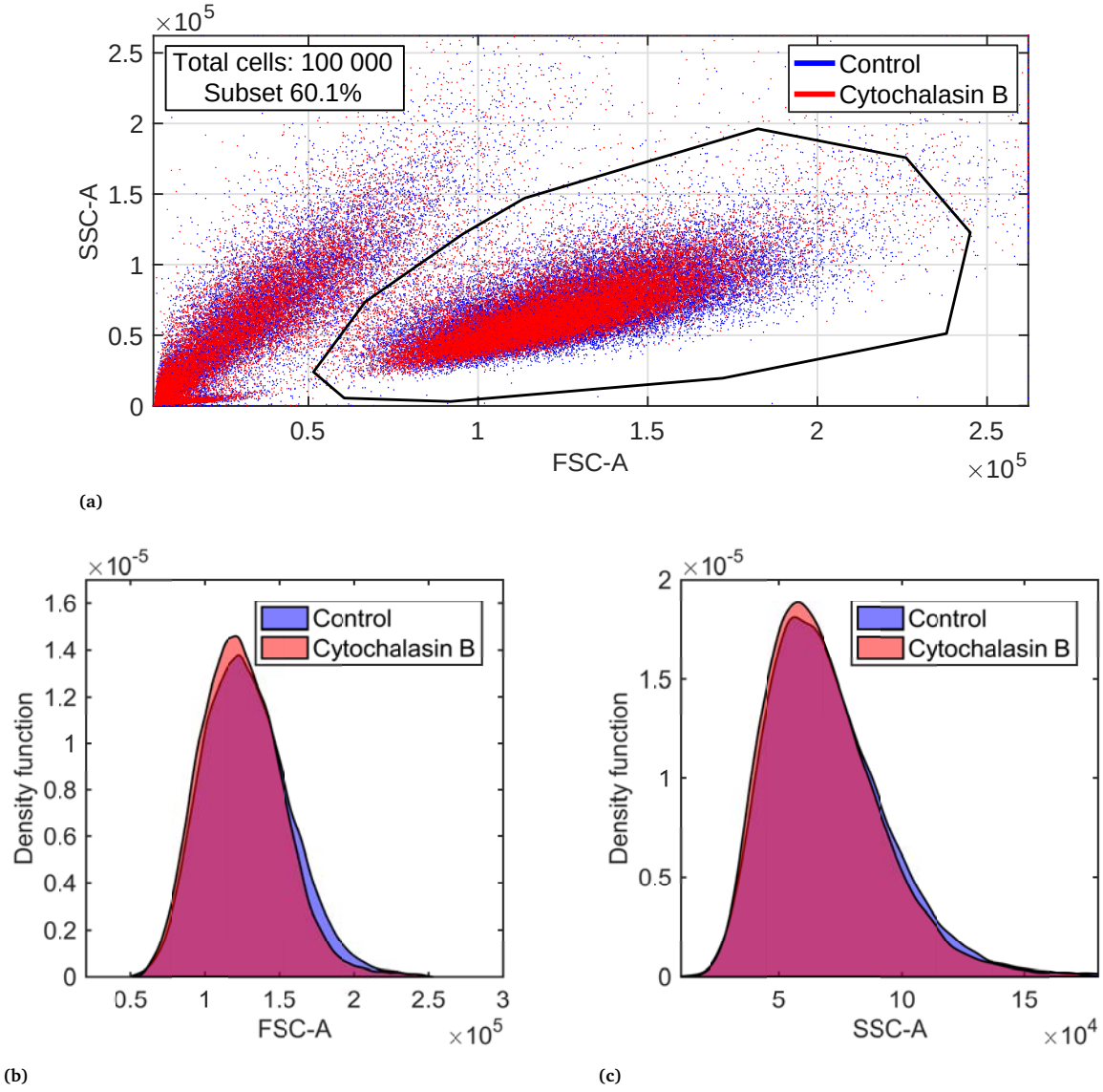

Fig. S6 Flow cytometry measurements of control and cytochalasin B treated HL-60 cells. (a) Flow cytometry FSC-A and SSC-A dot plot superimposition (2D OLR=1). (b) FSC-A histogram (1D OLR=1) and (c) SSC-A histogram (1D OLR=1) of subsets. One representative of at least two experiments.

Measured curve parameters dependencies to flow rate

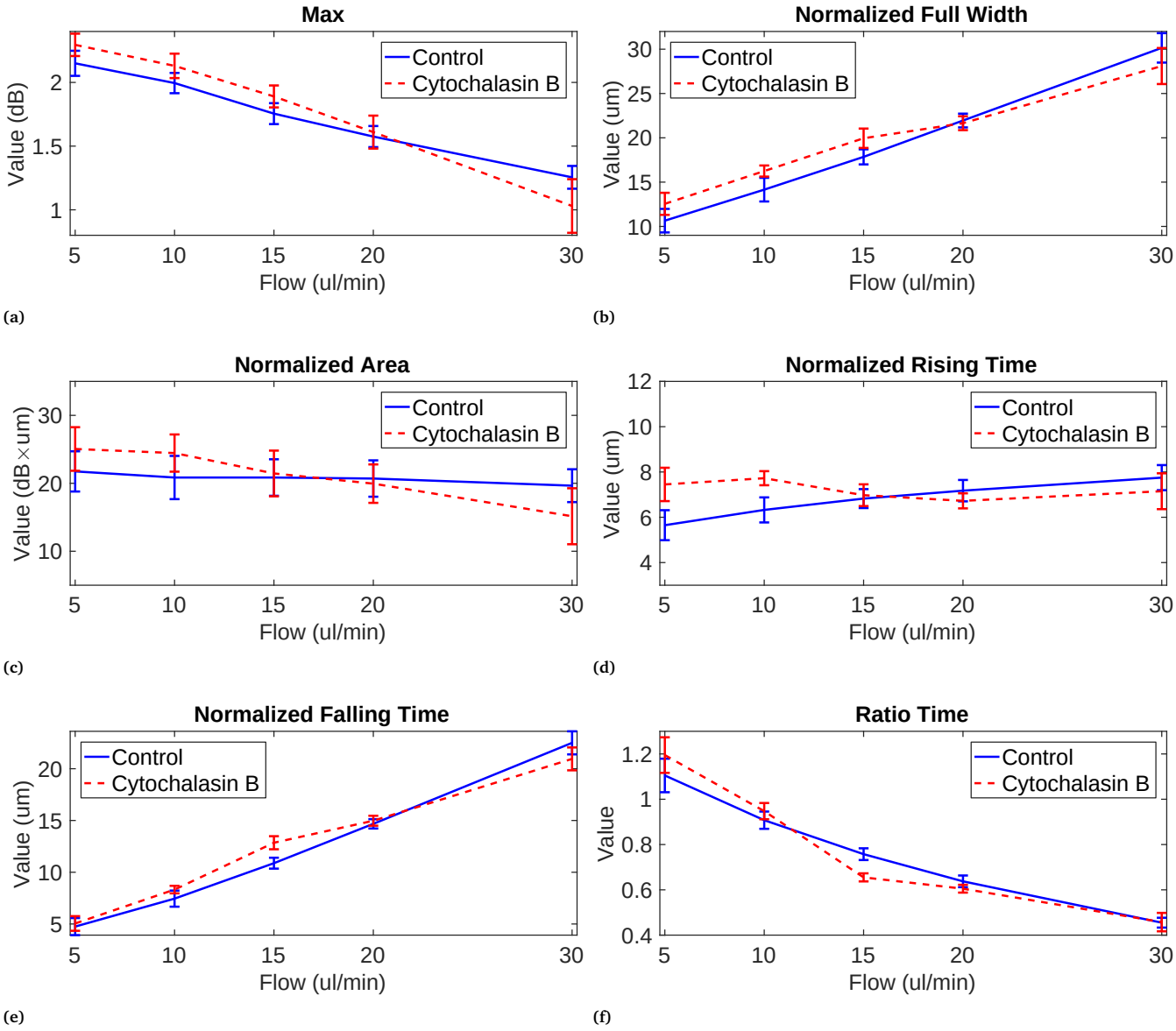

Fig. S7 Measured curve parameters dependencies to flow rate for (a) max, (b) full width (FW) normalized by velocity, (c) area normalized by velocity, (d) rising time (RT) normalized by velocity, (e) falling time (FT) normalized by velocity and (f) ratio time. Each error bar is $\pm$ one standard deviation derived from the normal distribution fitted over the corresponding parameter at a particular flow rate for a specific cell type. Parameters with time dependence, FW, area, RT and FT were multiplied by the particle velocity to represent values in terms of length rather then time. The total mode field diameter (MFD) of the fiber, or a fraction for RT and FT, was subsequently subtracted. Total number of cells and subset at each flow rate for control and Cytochalasin B treated HL-60 cells are reported in Tab. S3.

Larger flow rates implies larger forces acting on the cell thus more deformation is anticipated along the flowing direction. All parameters follow the predicted tendencies for both control and cytochalasin treated HL-60 cells (Fig. S4). Expectedly, FW values increase with increasing flow rates whereas max values decrease and normalized area values stay constant as shown in Fig.S7b, S7a and S7c respectively. Since the total effective RI volume (area) stays constant the volume ratio of the cell to the cavity is

smaller and thus yields smaller measured maximal RI variation (max). Variation of ratio time in function of flow rates reported in Fig.S7f shows decreasing values with increasing flow, rising time, Fig.S7d, shows relatively constant values whereas falling time, Fig.S7e, shows increasing values.

Interestingly, at a flow of 5 μl/min (particle velocity $U_p = 0.06$ m/s), both cell populations report signals yielding a ratio time value > 1. This indicates that the nucleus is positioned at the leading side of the cell rather than at the trailing side. At a flow of 10 μl/min ($U_p = 0.13$ m/s), the ratio time is very close to or slightly larger than 1, indicating near-symmetric RI distribution and a centered nucleus. For flows $>$ 15 μl/min ($U_p > 0.19$ m/s), ratio time values are < 1 indicating a nucleus positioned at the trailing side of the cell. These results suggest a transition between 5 and 15 μl/min for the nucleus to be placed at the leading or trailing side of the cell.

These flows coincide to particle Reynolds number $Re_p = Re(2R_{cell}/D_h)^2$ of 0.9 and 2.75 respectively, where Re is the channel Reynolds number and D_h is the hydraulic diameter of the channel. At $Re_p = 1$, namely the transition point between stokes and turbulent drag, the flow rate is 5.5 μl/min ($U_p = 0.07$ m/s). The transition of the particle Reynolds number from smaller to larger than 1 might be related to the ratio time transition, thus the relative position of the nucleus from trailing to leading. Indeed, a turbulent drag near the cell might promote the deformation of the membrane towards the leading side. Further investigation is required to confirm this theory.

Table S3 Total number of cells and subset at each flow rate for control and Cytochalasin B treated HL-60 cells.

	Control		**Cytochalasin B**	
	Total	**Subset**	**Total**	**Subset**
Q=5 μl/min	48 057	80.0%	45 835	75.4%
Q=10 μl/min	47 879	85.8%	36 518	54.9%
Q=15 μl/min	47 536	65.2%	50 759	62.8%
Q=20 μl/min	46 780	85.7%	51 081	46.6%
Q=30 μl/min	10 188	68.0%	49 864	85.7%

Derivation of particle velocities

The average particle velocity U_p is set to a fraction of the average fluid velocity in the microchannel $U_p = \gamma \times U_f$. The factor γ is experimentally derived as follows:

$$\gamma = \frac{U_p}{U_f} \qquad \text{where} \qquad U_f = \frac{Q}{W \times H} \qquad \text{and} \qquad U_p = \frac{D_{cell} + MFD}{\overline{FW}}$$

$$\gamma = \frac{D_{cell} + MFD}{\overline{FW} \times U_f} = \frac{(D_{cell} + MFD)(W \times H)}{\overline{FW} \times Q}$$

where Q is the flow rate, W and H are the channel width and height respectively, $D_{cell} = 12\ \mu m$ is the cell diameter, $MFD = 10.4\ \mu m$ is the mode field diameter of the SMF-28 optical fiber and $\overline{FW}$ is the average measured full width (FW) at the specific flow Q. This equation is valid for undeformed cells, at flows of 5 and 10 μl/min where the Ratio Time value is ≥ 1. At Q=5 μl/min in a $W = 40\ \mu m$ by $H = 15\ \mu m$ channel, $\overline{FW} = 3.37 \times 10^{-4}$ and yields a factor $\gamma = 0.48$ whereas at Q=10 μl/min, $\overline{FW} = 1.95 \times 10^{-4}$ and yields a factor $\gamma = 0.41$. Thus, the γ factor was set to an average of 0.45.

The theoretical derivation of the factor γ yields an equivalent value. Comparing the two forms of the particle Reynolds number Re_p:

$$Re_p = Re\left(\frac{D_{cell}}{D_h}\right)^2 \qquad \Leftrightarrow \qquad Re_p = \frac{\rho\,(U_f - U_p)\,D_{cell}}{\mu}$$

$$Re_p = \frac{\rho U_f D_h}{\mu}\left(\frac{D_{cell}}{D_h}\right)^2 \qquad \Leftrightarrow \qquad Re_p = \frac{\rho U_f\,(1-\gamma)\,D_{cell}}{\mu}$$

$$\gamma = 1 - \frac{D_{cell}}{D_h}$$

where $D_h = 2WH/(W+H)$ is the hydraulic diameter and ρ and μ are the fluid density and viscosity respectively. For the considered channel dimensions and cell diameter, $\gamma = 0.45$. Average fluid velocities, particle velocities, Re and Re_p calculated in a $W = 40\ \mu m$ by $H = 15\ \mu m$ channel at the different imposed flow rates using this factor are reported in Tab. S4. The same quantities in a $W = 30\ \mu m$ by $H = 15\ \mu m$ channel at a flow rate of 15 μl/min using $\gamma = 0.40$ are reported in Tab. S5.

Table S4 Calculated average fluid and particle velocities, Re and Re_p at the different imposed flow rates for $W = 40\ \mu m$, $H = 15\ \mu m$ and $D_{cell} = 12\ \mu m$ using $\gamma = 0.45$.

Flow rate Q (μl/min)	5	10	15	20	30
Fluid velocity U_f (m/s)	0.14	0.28	0.42	0.56	0.83
Reynolds number (Re)	3	6	9	12	18
Particle velocity U_p (m/s)	0.0625	0.125	0.1875	0.25	0.375
Particle Reynolds number (Re_p)	0.9	1.8	2.75	3.7	5.5

Table S5 Calculated average fluid and particle velocities, Re and Re_p at a flow rate of 15 μl/min for $W = 30\ \mu m$, $H = 15\ \mu m$ and $D_{cell} = 12\ \mu m$ using $\gamma = 0.40$.

Flow rate Q (μl/min)	15
Fluid velocity U_f (m/s)	0.56
Reynolds number (Re)	11
Particle velocity U_p (m/s)	0.22
Particle Reynolds number (Re_p)	4.0

Coefficients of variation (CV) of flow cytometry and RIC measurements

Table S6 Calculated coefficients of variation of FSC-A and SSC-A measurements for control and Cytochalasin B treated HL-60 cells.

	FSC-A	SSC-A
Control	22.6%	34.7%
Cytochalasin B	21.8%	33.8%

Table S7 Calculated coefficients of variation of Max, FW, Area, RT, FT and Ratio Time measurements for control and Cytochalasin B treated HL-60 cells at all flow rates.

	Flow rate Q (μl/min)	Max	FW	Area	RT	FT	Ratio Time
Control	5	10.6%	7.5%	17.5%	9.8%	13.6%	14.8%
	10	7.9%	6.8%	16.1%	7.6%	8.3%	8.0%
	15	7.5%	5.4%	15.6%	5.6%	6.8%	6.4%
	20	7.8%	3.8%	14.6%	5.8%	3.8%	5.5%
	30	9.6%	4.2%	14.0%	7.1%	5.4%	9.7%
Cytochalasin B	5	4.9%	6.6%	12.6%	7.7%	9.5%	9.6%
	10	8.2%	3.6%	13.9%	4.0%	5.4%	6.1%
	15	14.0%	5.4%	22.3%	6.0%	5.5%	3.6%
	20	18.9%	4.0%	22.7%	4.3%	4.6%	4.2%
	30	22.1%	6.2%	29.1%	10.3%	7.0%	11.5%

Table S8 Calculated coefficients of variation of FSC-A and SSC-A measurements for neutrophils, basophils and baseline conditions.

	FSC-A	SSC-A
Neutrophils	13.2%	23.2%
Basophils	15.6%	29.9%
Baseline	15.7%	30.4%

Table S9 Calculated coefficients of variation of Max, FW, Area, RT, FT and Ratio Time measurements for neutrophils, basophils and baseline conditions at a flow rate of 15 μl/min.

	Max	FW	Area	RT	FT	Ratio Time
Neutrophils	9.2%	5.7%	12.8%	7.6%	5.0%	5.1%
Basophils	9.4%	4.0%	13.3%	4.5%	4.1%	2.5%
Baseline	11.8%	8.4%	16.8%	8.6%	8.4%	3.2%

OLR of myeloid cells populations

Table S10 Calculated 1D OLR values of all combinations of myeloid cells for discrimination.

	Neutrophils vs Basophils	Neutrophils vs Baseline	Basophils vs Baseline
Max	1	1	1
Full width (FW)	1	0.91	1
Area	1	0.90	1
Rising time (RT)	0.98	0.83	1
Falling time (FT)	1	1	0.998
Ratio time	1	1	1

1D OLR are not smaller than 1 in all cases. However, using the right combination of parameters, cell populations can be easily discriminated. Indeed, OLR computed in 3D using the FW, RT and FT are all below 1 (3D OLR neutrophils-basophils=0.41, neutrophils-baseline=0.82 and basophils-baseline=0.66).

References

1 J. Zhou and I. Papautsky, *Lab on a chip*, 2013, **13**, 1121–32.

2 D. Di Carlo, *Lab on a Chip*, 2009, **9**, 3038–3046.